



## **Lightning activity seen by GLD360 measurements and MTG satellite observations in relation to occurrence of extreme weather**

**Christo G. Georgiev<sup>1\*</sup>, Ján Kaňák<sup>2</sup>, Gerrit Holl<sup>3</sup>**

<sup>1</sup> *National Institute of Meteorology and Hydrology,  
Tsarigradsko shose 66, 1784 Sofia, Bulgaria)*

<sup>2</sup> *Slovak Hydrometeorological Institute  
Jeséniova 17, 851 07 Bratislava, Slovakia*

<sup>3</sup> *Deutscher Wetterdienst)  
63067 Offenbach am Main, Germany*

**Abstract:** Lightning data derived by the Lightning Imager (LI) on board of Meteosat Third Generation (MTG) satellites are analyzed in relation to extreme weather events in a case study over Bulgaria on 3 October 2025. Time series of flash detection by the MTG LI instrument are used to study the link between lightning activity and severe weather near specific points, where data from meteorological observations are available. RGB analyses are performed to reveal details of the thunderstorm cloud systems and to identify the position of lightning activity within the convective cloud structure. Considering Flash Density parameter provides useful information to distinguish areas of convection, associated with moderate and extreme precipitation and thus to anticipate the severity of the thunderstorms. Methodology for analyses based on data from Global Lightning Detection network GLD360 is also presented considering the case of severe convective storms over Germany on 20 June 2013. An approach for identifying lightning jumps is proposed to study the association of rapid increase of lightning activity with severe phenomena produced by the thunderstorms.

**Keywords:** Remote sensing, Lightning, Meteosat, GLD360, Severe Convection

---

\* Christo.Georgiev@meteo.bg

## **1. INTRODUCTION**

The new Lightning Imager (LI) instrument of Meteosat Third Generation (MTG) satellite performs continuous observations of lightning activity from space, providing comprehensive data on lightning flashes across Europe and Africa for the first time (EUMETSAT, 2025a). Efforts of user community for scientific understanding and meteorological interpretation of these new valuable MTG data have been initiated before the launch of MTG. In 2020 EUMETSAT, the European Organisation for the Exploitation of Meteorological Satellites has generated Test LI Level 2 (L2) Dataset simulated at EUMETSAT that corresponds to a real meteorological situation of the date 20 June 2013. This date was carefully selected by meteorologists in EUMETSAT and the European Severe Storm Laboratory (ESSL) based on the forecast of severe weather situation and appearance of convective storms over Germany. After the successful launch of MTG and its commissioning, real time LI L2 products are operationally distributed to the users since 31 October 2024. Still during the commissioning phase of MTG LI instrument various studies have been performed to infer the prospects which the new MTG LI data offers for nowcasting convective storms. Based on the first results it was reported for a solid evidence that LI data can improve the forecasting of hail, while the identification of an elevated potential for heavy rain, convective wind events, and tornadoes, needs to be further examined (EUMETSAT, 2025b).

Our work is focused on the occurrence of severe weather events like heavy precipitations and wind gusts in connection with the evolution of lightning activity as seen by remote sensing data. Two types of lightning data are considered in cases of large scale weather systems with embedded thunderstorms developed in environment of strong upper-level dynamics:

- Data from measurements of Global Lightning Detection network GLD360, presented in terms of simulated MTG LI Level 2 Flash (LFL) product for 20 June 2013 over Central Europe, used in the study presented in Section 2.
- Real time LI L2 information for 3 October 2025 over South-Eastern Europe, processed operationally and used as a data source in Section 3.

The study is a part of the activities in EUMETSAT and in the National Institute of Meteorology and Hydrology (NIMH) of Bulgaria for preparation of using data from LI instrument of MTG satellite. Visualization of MTG data in this paper is made using GEOProc Software developed by the second author and provided to NIMH for operational use and research applications.

## **2. THUNDERSTORM ACTIVITY OVER GERMANY ON 20 JUNE 2013 AS SEEN IN DATA FROM GLD360 MEASUREMENTS**

### **2.1. The severe weather situation**

On 20 and 21 June 2013, the area along a cold front developed over Eastern Europe experienced extremely bad weather in the form of thunderstorms with large hailstones,

*Lightning activity seen by GLD360 measurements and MTG satellite observations in relation to occurrence of extreme weather*

extensive heavy rain and strong wind gusts (DWD, 2023). Figure 1 shows the associated cloud system on 20 June at 0900 and 1900 UTC seen in Air Mass RGB (WMO, 2025) composed from experimental 2.5-minutes Super rapid-scan (RSS) measurement by Meteosat Second Generation (MSG) satellite (EUMETSAT CWG, 2013). The stratospheric intrusion of dry air in its rear side (reddish color), favors the convective development ahead. The lightning activity is illustrated in the image with flashes accumulated in time interval 60 minutes, red color is for the oldest flashes, yellow for the newest. Also indicated in Figure 1b the location of some meteorological observations over the area considered in this study. These are locations of severe weather events as described in Table 1 and Table 2 according to the records of Deutscher Wetterdienst (DWD).

The lightning activity and evolution is considered in two aspects:

- Evolution of the number of flashes in time associated with convective thunderstorm systems by tracking along the line of severe weather reports in order to study the severe weather occurrence in association with substantial and rapid increase in lightning activity.
- Time series of the number of flashes at locations of severe weather reports in order to anticipate the severe weather occurrence related to increasing lightning.

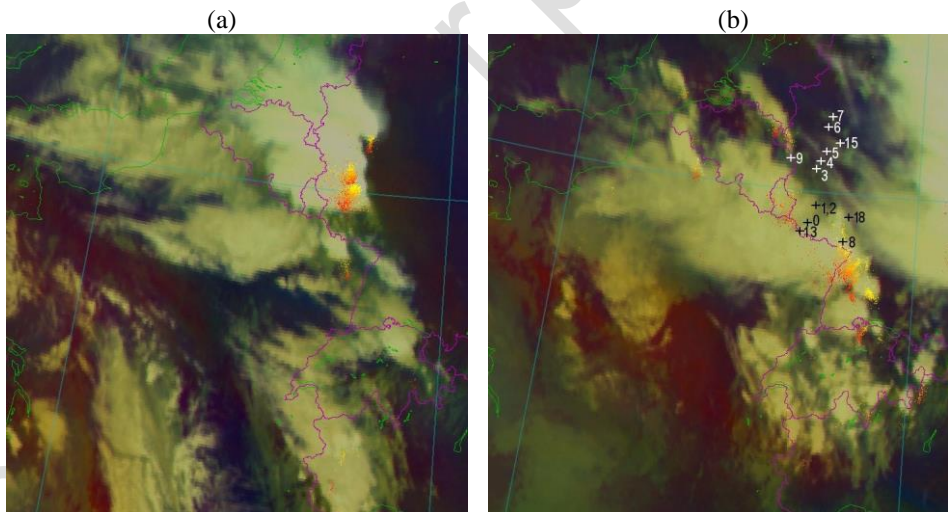


**Fig. 1.** Air Mass RGB composition of MSG channels on 20<sup>th</sup> of June 2013 (a) at 0900 UTC; (b) at 1900 UTC with lightning accumulated in time interval 60 min (from red color for the oldest flashes to yellow for the newest). Also indicated in (b) the location of the observations of severe weather shown in Table 1 and Table 2.

**Table 1.** Some heavy rain locations.

Time period	Location name	Rain	Longitude °E	Latitude °N	Index
06 – 07 UTC	Schmelz-Hüttersdorf	31 mm	6.85	49.43	0
06 – 07 UTC	Deuselbach	42 mm	7.05	49.76	1
08 – 09 UTC	Deuselbach	33 mm	7.05	49.76	2
09 – 10 UTC	Kaltenborn-hochacht	32 mm	6.99	50.39	3
10 – 11 UTC	Bad Neuenahr, Ahrweiler	41 mm	7.09	50.53	4
10 – 11 UTC	Bonn-Roleber	46 mm	7.19	50.73	5
11 – 12 UTC	Remscheid-Lennep	55 mm	7.25	51.18	6
11 – 12 UTC	Gevelsberg-Oberbroeking	45 mm	7.34	51.33	7
19 – 20 UTC	Bad Bergzabern	40 mm	7.00	49.11	8
20 – 21 UTC	Monschau-Kalterberg	48 mm	6.25	50.53	9

**Table 2.** Some wind gusts locations.

Time period	Location name	Wind	Longitude °E	Latitude °N	Index
07 – 08 UTC	Berus	22 m/s	6.69	49.26	13
10 – 11 UTC	Nuembrecht	28 m/s	7.55	50.91	15
19 – 20 UTC	Weinbiet	31 m/s	8.12	49.38	18

## 2.2. Tracking methodology

A simple Tracking algorithm is applied: A start position of the storm and its end position are manually determined on the satellite images. The background map is generated from MSGProc software in Albers equal-area projection with 3 km pixel size. Coordinates  $x,y$  from satellite Geoview projection are used to calculate real geographical coordinates and in next step are re-calculated to  $X,Y$  coordinates inside the background image in subarea of  $900 \times 700$  pixels. Then the storm positions in 2.5 min time intervals between start  $(X_0, Y_0)$  and final  $(X_1, Y_1)$  points of a desired storm track are identified to determine the intermediate positions of the thunderstorm along the track, as illustrated in Figure 2.

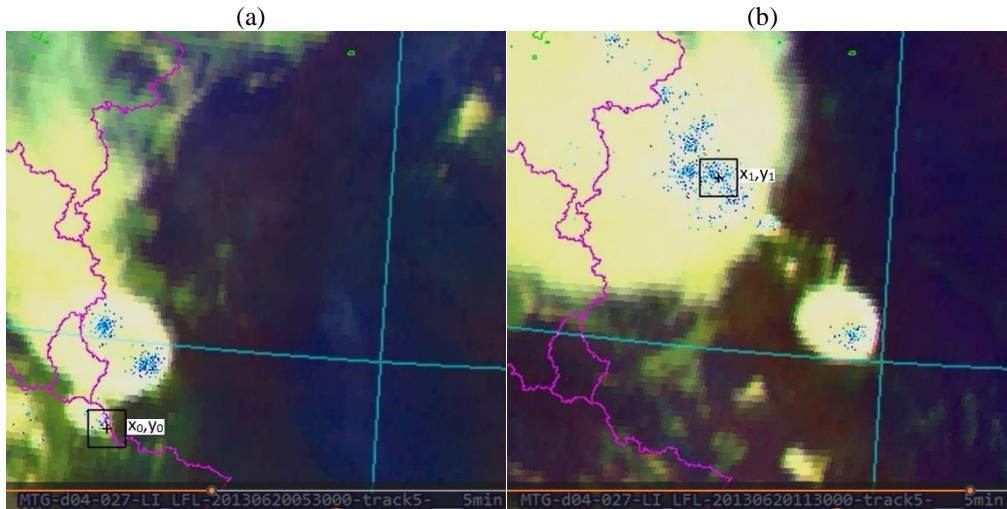


**Fig. 2.** Start  $(x_0, y_0)$  and final  $(x_1, y_1)$  thunderstorm position between 0530 and 1130 UTC on 20<sup>th</sup> of June 2013 along a line near stations No 13, Berus and No 6, Remscheid-Lennep. Air Mass RGB overlaid by 10 sec GLD360 flash data in 10 minutes accumulations, newest flashes in cyan, oldest flashes in blue.

Detections of flash events by GLD360 measurements collected within time windows of 10 sec are used as a parameter to represent the lightning activity. Accumulated flash counts in 2.5 min intervals are extracted over areas of  $25 \times 25$  pixels box around the center of the storm position at each point of the track. Such a processing enables to catch relevant number of flash data for the selected storm during the tracking and give the opportunity to identify lightning jumps when the trajectory is not linear.

A Lightning Jump is detected in case of substantial and rapid increase in lightning activity in a tracked thunderstorm cell.

In addition, number of flashes are calculated in square of approximately  $20 \times 20$  km per minute averaged from 60 min accumulated data in different steps of minutes for the periods of time around the severe weather report time.

### **2.3. Lightning activity evolution and severe weather occurrence**

To study the relation between Flash activity and severe weather reports the geographical coordinated of the weather stations are converted to X, Y subarea coordinates in Albers projection. Then the time when the thunderstorm develop near a weather station along the storm track is approximately determined as it is indicated by magenta arrows in Figure 3a.

Figure 3a shows that lightning activity intensifies prior or at the beginning of the period of severe weather events near the location of meteorological stations Schmelz-Hüttersdorf with heavy rain above 30 mm/h reported and Nuembrecht wind gusts 28-30 m/s measured.

Figure 3b shows trajectory of another track and the number of flashes detected by GLD360 instrument in time. It confirms that the peak of lightning activity seen near the location of Deuselbach (7.05 °E, 49.76 °N and subarea coordinates X=569, Y=923) is followed by 42 mm rain from 06 to 07 UTC measured at this weather station.

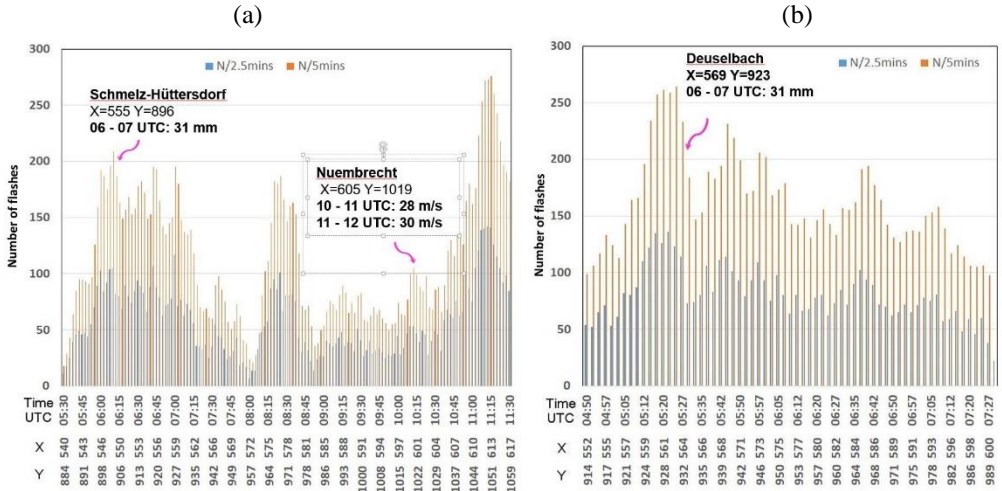


**Fig. 3.** Time series of lightning activity on 20<sup>th</sup> of June 2013 (a) along a track over Germany with heavy rain and wind gusts indicated at 2 weather station; (b) along a track passing near meteorological station Deuselbach with heavy rain reported during 2 hours around 07 UTC.

Association of rapid increase of lightning activity with severe phenomena produced by the thunderstorms is well illustrated in Figure 4, which shows 10-seconds GLD360 data from the morning on 20<sup>th</sup> of June 2013 until midnight at weather stations No 6, Remscheid-Lennep (gray curve) and No 18, Weinbiet (blue curve). It appears that two lightning jumps seen in Figure 4a are related to severe weather according to the reports in Table 1 and Table 2. They correspond to extreme weather reported, as follows:

- Rain of 55 mm in the period from 11 to 12 UTC at Remscheid-Lennep, location 7.25 °E, 51.18 °N corresponds to Jump 1 between 1030 and 1200 UTC.
- Wind gusts of 31 m/s between 19 and 20 UTC at Weinbiet, location 8.12 °E, 49.38 °N is related to Jump 2, which appears in the period 1930 – 2030 UTC.

*Lightning activity seen by GLD360 measurements and MTG satellite observations in relation to occurrence of extreme weather*

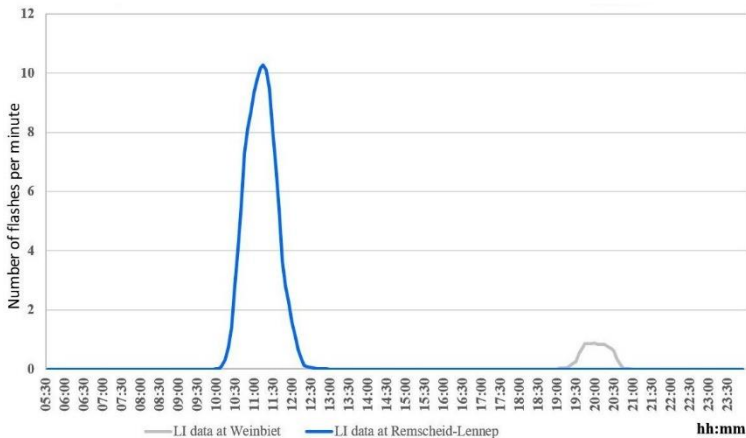


**Fig.4.** Number of GLD360 flash values in square approximately 20×20 km per minute averaged from 60 minutes accumulated data, normalized to the number of flashes per minute along a track over Germany with heavy rain and wind gusts indicated at 2 weather station on 20<sup>th</sup> of June 2013.

Figure 5 provides another sort of analysis applied by considering the number of flashes detected by GLD360 instrument related to a storm trajectory/track in a period around the corresponding pass time near severe weather locations.

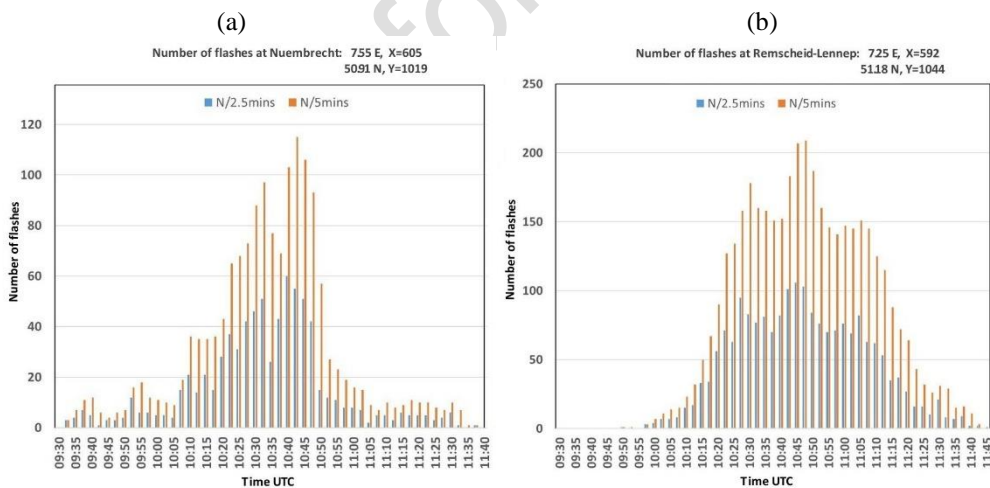


**Fig. 5.** Time series of lightning activity on 20<sup>th</sup> of June 2013 (a) At weather station Nuembrecht where rain of 28 m/s are measured between 10 and 11 UTC; (b) at weather station Remscheid-Lenep where rain of 55 mm is measured for 1 hour from 11 to 12 UTC.

Figure 5a shows that wind gusts of 28 m/s are measured at weather station Nuembrecht between 10 to 11 UTC and in the same time the number of flashes

significantly increases after 1020 UTC. In Figure 5b the period from 11 to 12 UTC, when heavy rain of 55 mm was measured at weather station Remscheid-Lennep, lies 15 minutes after the maximum in the number of flashes detected at the position of the station location.

Considering these four events it seems that in association with moving thunderstorms, wind gusts appear in the early stages of lightning activity, while some lead time seems to be needed after the lightning jump for heavy rain to occur. It is worth mentioning that according to the experience among the community the lightning jump signal in itself is a very difficult topic, and one should be quite careful in conclusions on this topic.

### **3. REAL TIME MTG LI DATA IN THUNDERSTORM ACTIVITY OVER BULGARIA ON 3 OCTOBER 2025**

Since 31 October 2024 MTG-II satellite provides a real time lightning detection and location of (cloud-to-cloud and cloud-to-ground with no discrimination between them). Figures 6a and 6b shows MTG images in 6.3  $\mu\text{m}$  water vapor (WV) channel over Eastern Europe, overlaid by LFL lightning counts, accumulated in the previous of last 2 hours. The oldest flashes are represented in reddish colors, while the newest ones with yellowish colors.

#### **3.1. Association of lightning activity to circulation and related weather patterns**

The water vapor channel imagery analysis shows a typical flow pattern of strong meridional blocking over Eastern Europe, in which the air moves north and south having large amplitude with a deep trough and peaked ridges on its two sides (Stoyanova and Georgiev, 2013). As seen in Fig. 6a, the related jet stream exhibits a highly amplified trough feature, seen as a corresponding large amplitude moisture boundary in the satellite WV image on both side of the dark dry zone over Italy. This is a sign for strong intrusion of dry polar air and vorticity embedded through the jet into the circulation of the upper-level low that tends to be blocked over the Eastern Mediterranean. In this synoptic situation, rapid cyclogenesis has occurred in the Central/Eastern Mediterranean. The baroclinic trough feature in Figure 6a has been rapidly transformed for 12 – 15 hours into a spiral pattern associated with revolution of the dry intrusion around the upper-level cyclonic circulation, seen in Figure 6b. It has been shown that the spiral patterns commonly developed after the surface deepening had nearly finished, and the upper-air cyclone continued to intensify, or maintained its strength (Georgiev et al., 2016).

*Lightning activity seen by GLD360 measurements and MTG satellite observations in relation to occurrence of extreme weather*

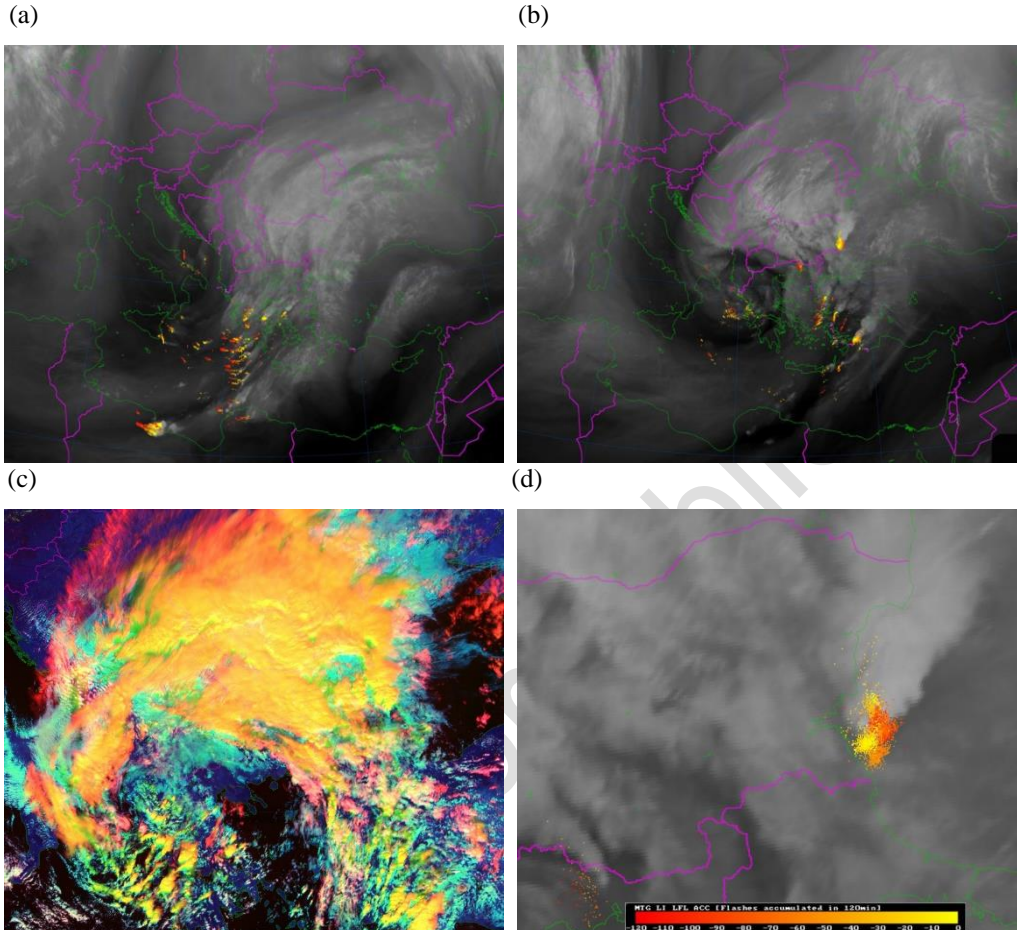


**Fig. 6.** MTG images in 6.3  $\mu\text{m}$  WV channel with accumulated over 120 min LFL counts (oldest in reddish, newest in yellowish colors) (a) on 2<sup>th</sup> of October 2025 1500 UTC] (b) and (d) on 3 October 2025 0600 UTC; (c) Day Cloud Type RGB on 3 October 2025 0600 UTC. Also shown in (d) the color palette used in (a), (b) and (d).

This is a typical situation for this geographical region in October when the warm water of Mediterranean basin is a source of low-level thermal advection and/or latent heat release through convection. These processes contribute to cyclogenesis by inducing low level pressure falls, amplifying the upper-level wave and creating a feedback aloft as the surface cyclone strengthens. As a result, mutual interaction of the disturbances at the tropopause and the surface occurs. The related mechanisms, broadly presented in the literature and discussed by Stoyanova and Georgiev (2013), contribute to an increase of horizontal moisture flux. In combinations with increase in moisture flux convergence at the Black Sea coast all these factors play critical role for extreme inland precipitation over the region of southeastern Bulgaria.

Figure 6a and Figure 6b show that thunderstorms develop in association with the cold front systems and near the Black Sea coast, where the induced lifting and moist warm sea surface air contribute to convective initiation and rapid development of deep moist convection. The Day Cloud Type RGB (see WMO, 2025) derived as a combination of the observations of near infrared and visible channels of FCI instrument onboard of MTG-II is shown in Figure 6c. The cloud analysis reveals mostly multilayered thick clouds with ice on the top (yellow colors), including over Bulgaria in the northeastern diffluent part of the cyclone. Considering only the cloud field in Figure 6c it is impossible to determine where extreme weather is likely to occur and taking into account the considerations in Section 2, LI data would be useful to identify such areas of potential severe weather.

Figure 6d is a zoom of WV image in Figures 6b at the Black Sea coast on 3 October 2025 0600 UTC showing the vigorous convective system. Considering the LFL data patterns in Figures 6a and 6d, the difference in their structure is related to the circulation pattern and provides information for the development of convective system:

- In Figure 6b fast moving thunderstorms associated with a cold front system exhibit distinct separation between old flashes (in red) in the rear side of convective system and newest flashes (in yellow) on its leading part.
- Since the thunderstorms in Figure 6d develop in persistent convective environment of the blocking regime, the areas of old flashes (reddish colors) and newest flash occurrence (in yellow) are mixed. This is a sign for regeneration of convection from low-level at the same place due to the persistent nature of the blocking circulation.

Section 3 is focused on the link of lightning activity to heavy rain events near the Black Sea coast measured by the Synoptic Station at Emine Cape (No 15650, 42.70 °N, 27.90 °E) and Automatic Meteorological Stations (AMS) of NIMH in Nesebar (No 28740, 42.66 °N, 27.74 °E) as well as inland at AMS Beloslav (No 27460, 43.19 °N, 27.70 °E) and AMS Sindel (No 27480, 43.11 °N, 27.60 °E). In Figure 7a the location of the synoptic station Emine and the three AMS meteorological stations are indicated with their numbers, also shown the accumulated flashes on 3 October at 0600 UTC during the previous 60 minutes superimposed on HRV-clouds RGB (FCI channels 0.6  $\mu\text{m}$  on the red and green beams and 10.5  $\mu\text{m}$  on the blue beam). To check on the association of this lightning activity to extreme weather, Figure 7b shows the hourly accumulated precipitations during the same period derived from satellite observations. H61 product of EUMETSAT Satellite Application Facility on Support to Operational Hydrology and Water Management (H-SAF) is considered, since data from radar measurements are not available. Extremely strong lightning activity is related to the core of the deep convection about 10 km in the water area of Black Sea, where the heaviest rain was measured (near stations 15650 and 27460). MTG LI instrument has detected much less flashes to the north (near AMS 15650 and 27460), where lower rain quantities are seen in Figure 7b accordingly.

*Lightning activity seen by GLD360 measurements and MTG satellite observations in relation to occurrence of extreme weather*

Parallax correction is not performed on the lightning data as well as on the MTG FCI images, so qualitative comparison of Figures 7a and 7b can be made without any considerations regarding this effect, although H61 product is corrected for parallax shift.

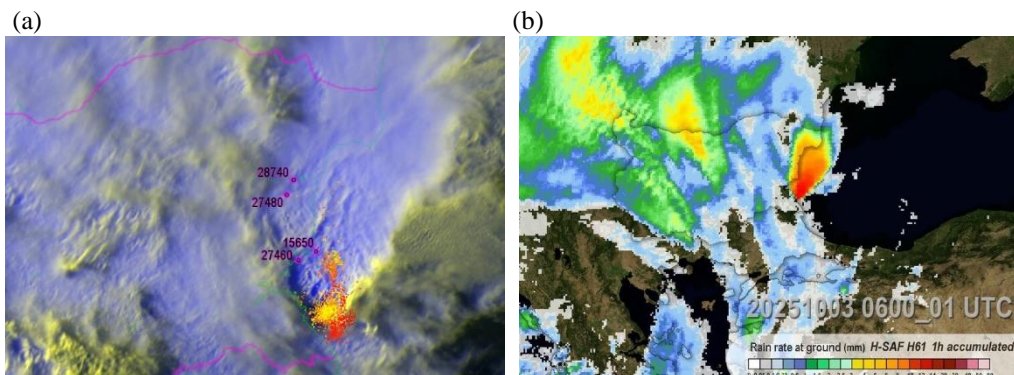


**Fig. 7.** (a) HRV-clouds RGB image with accumulated flashes (LFL counts) over 60 min (oldest in reddish, newest in yellowish) on 3<sup>rd</sup> of October 2025 at 0600 UTC; (b) The corresponding satellite observations of hourly precipitations from 05 to 06 UTC according to HSAF H61 product.

### 3.2. Lightning activity versus rain quantities and cloud analyses

For a better interpretation, the Flash Density is considered as number of MTG LI LFL counts per square meter per hour during shorter to larger periods (5 min to 120 min). In GEOView software the values of this parameter are calculated in square 5×5 pixels of the Albers projection. In our study we use a projection map with "scale factor" 0.5, which represents pixel size in km, that means representation of Flash Density in 2.5×2.5 km grid. In Figure 8, the Flash Density is superimposed on a sequence of FCI HRV-clouds RGB, one hour later around a period of strengthening precipitations over the two weather stations.

Quantitative data for precipitations are shown in Table 3 according to H61 product with resolution about 5 km over Bulgaria, corrected for parallax error (H-SAF, 2024).

**Table 3.** Hourly quantities of rain (mm) measured at AMS Nesebar and near its location derived from satellite observations according to H-SAF H61 product on product 3<sup>th</sup> of October 2025.

Data Source	0600 UTC	0700 UTC	0800 UTC
AMS Nesebar	9.0	13.9	14.9
MSG H-61, inland, 27.68 °E, 42.66 °N, 5.025 km west of AWS Nesebar	4.0	3.0	2.5
MSG H-61 coastal water area 27.86 °E, 42.70 °N, 10.76 km northeast from AWS Nesebar and 3.58 km west of Emine	9.30	5.4	5.10

Analysis of Figure 8 shows that the most active lightning area is not in the same location, but a bit more than 10 km from the location of the automatic meteorological stations Nesebar (with parallax correction approximately taken into account).

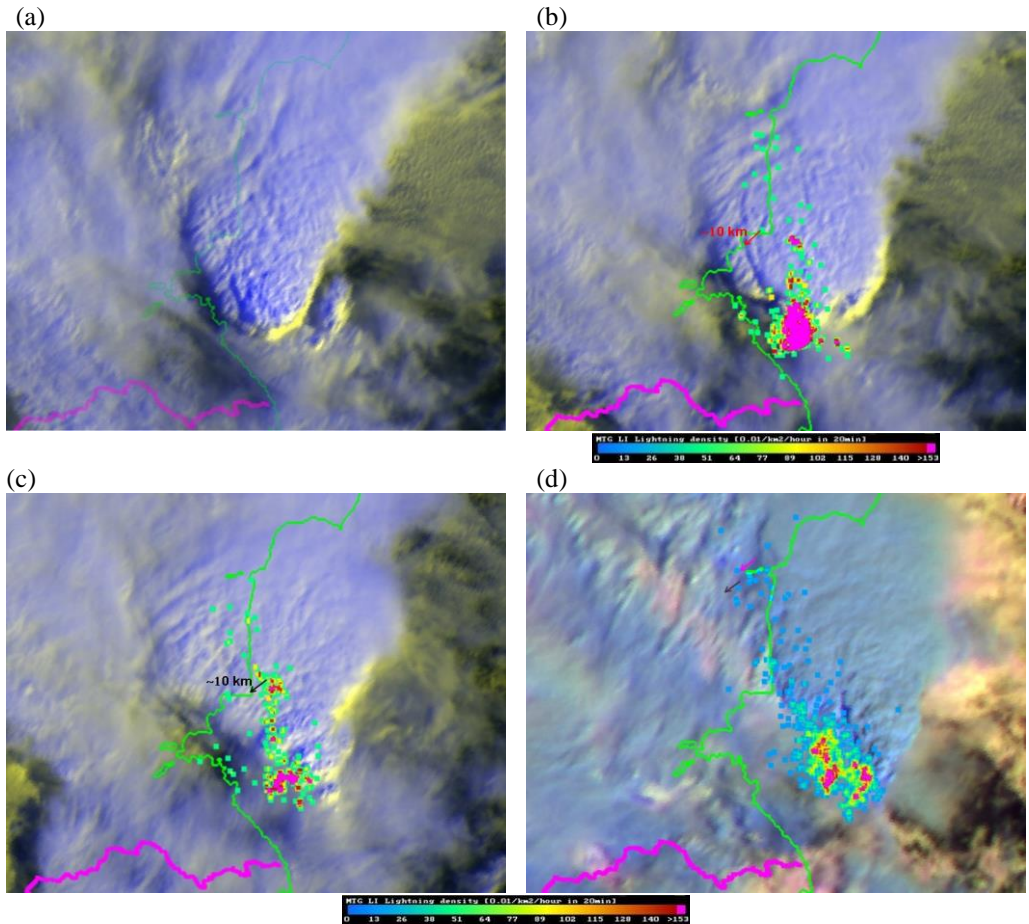


**Fig. 8.** HRV-clouds RGB on 3<sup>th</sup> of October 2025 at (a) 0620 UTC and with Flash Density [0.01/km<sup>2</sup>/hour in 20 min] overlaid at (b) 0640 UTC, (c) 0710 UTC and (d) 0840 UTC. Black and red arrows indicate approximate location of Cape Emine and AMS Nesebar, and the arrows' length corresponds to the distance of about 10 km to be applied for LFL parallax collection in southwest direction.

**Table 4.** Quantities of rain (mm) measured each ten minutes at AMS Nesebar on 3 October 2025.

	0640 UTC	0650 UTC	0700 UTC	0710 UTC	0720 UTC	0730 UTC
Rain, mm	0.8	1.2	4.8	7.1	3.3	1.4

The data in Table 4 however confirm that the propagation of the convective cloud system and detection of single flashes in the vicinity of AWS Nesebar (Figures 8a, 8b

*Lightning activity seen by GLD360 measurements and MTG satellite observations in relation to occurrence of extreme weather*

and 8c) is associated with heavy rain of 15.2 mm for half an hour measured at AMS Nesebar from 0650 UTC to 0720 UTC.

In October with lower zero-degree isotherm height over this region, ice particles and semi-frozen water drops (graupel) may be formed at an early stage when the convection process still operates from the surface up to middle troposphere. As a result, mid-level thunderstorm clouds are built with lightning activity near the environment of convective initiation. Such a thunderstorm rapidly developed around 11 UTC near synoptic station at Cape Emine.

For cloud analysis, three types of RGB compositions are presented in Figure 9. In Figure 9 (a), high Flash Density in time period of 5 minutes is seen at 1050 UTC within multilayered thick clouds with ice on the top (yellow colors of Day Cloud Type RGB). Ten minutes later (Figure 9b) this area of lightning activity is surrounded mostly by cyan colors in the Day Cloud Phase RGB image that is a sign for thick ice clouds, small particles. Flashes are not detected by MTG LI in the anvil of high clouds (greyish in HRV-clouds RGB, Figure 9d). This is in agreement with the conclusion in EUMETSAT (2025b) that flashes occur especially with updrafts that produce small ice crystals in their anvils (light blue in the Day Cloud Phase RGB). Figure 9b shows that from south to north, the predominant cyan/light blue color of the convective system increasingly acquires darker blue hues, indicating mainly large ice particles on the cloud top.

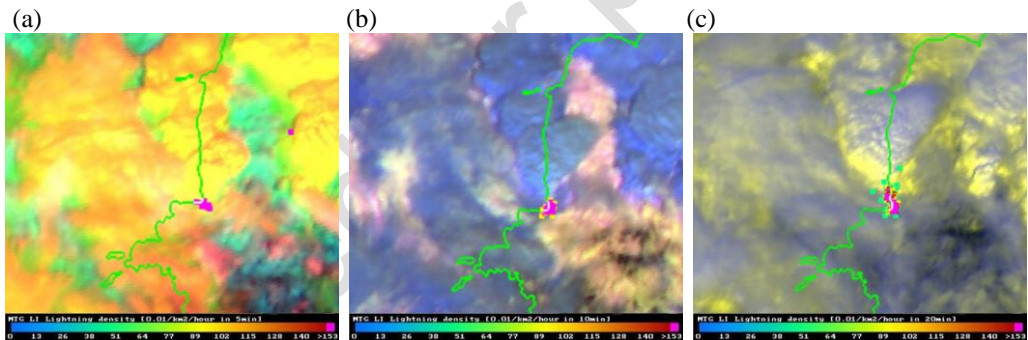


**Fig. 9.** Mid-level thunderstorm development on 3<sup>th</sup> of October 2025 seen in MTG FCI imagery: (a) Day Cloud Type RGB, 1050 UTC, Flash Density [0.01/km<sup>2</sup>/hour in 5 min]; (b) Day Cloud Phase RGB, 1100 UTC, Flash Density [0.01/km<sup>2</sup>/hour in 10 min]; (c) HRV-clouds RGB, 1110 UTC, Flash Density [0.01/km<sup>2</sup>/hour in 20 min].

The instant lightning activity occurs only close to the area of convection initiation near the sea water area. Such kind of lightning activity was reported in EUMETSAT (2025b) regarding two of the application studies of mesoscale convective systems (Eastern Spain, Balearic Sea on 3 September 2024 as well as Bosnia, Herzegovina on 3-4 October 2024). Such kind of storms over the region tend to produce enormous anvil area due to the high CAPE in the inflow of the storms (near sea coast areas) and cold Equilibrium level (at lower zero-degree isotherm height). As shown in EUMETSAT (2025b) and seen in Figure 9, LI data are helpful to show that the active part of the storm

may remain closely associated only with the southern flank of the large anvil and the other parts of the anvil may not involve active convective cores.

It is notable the difference between the two convective processes considered in this section that have been developed within 4 hours on 3<sup>th</sup> of October 2025. The thunderstorm at the Black Sea coast around 11 UTC appears in the HRV-clouds RGB on Figure 9c with mid-level clouds (yellow RGB shades). The other convective cloud system developed four hours earlier mainly over the sea water (Figure 8) but with inland lightning activity to the west, exhibits greyish and blueish colors mostly that are indicative of high clouds.

Another characteristic only of the process seen in Figure 9 is that the flash activity is closely associated with the area of low-level convection and progressively disappears along the propagation to the north of the convective cloud system as a V-shape feature. This is likely to be a result of insufficient number of ice particles/graupel far from the environment of convection initiation due to less favorable thermodynamic and moisture conditions of the environment.

### 3.3. Flash Density evolution and extreme precipitation

Based on hourly data from ground measurements and synoptic observations, this section is focused on the possibility to use Flash Density as a parameter related to the occurrence of extreme precipitation over the area around the meteorological stations in Table 5.

The presented accumulated rain quantities—hourly around 08 UTC and three-hourly at 09 UTC—are associated with the storm, shown in Figure 7 and Figure 8 developed mainly over the sea water area. Although the AMS Beloslav and AMS Sindel are located out of the main convective cloud system, extreme precipitations around 08 UTC are related to lightning activity seen through the Flash Density parameter on Figure 8d. Also, the analysis shows slightly higher 3-hourly precipitation accumulation from 06 to 09 UTC at Emine, which is located nearer to the active lightning area than Nesebar, and close to the flash area as seen in Figure 8 (assuming parallax correction as well).

**Table 5.** Hourly and three hourly quantities of rain (mm) measured at synoptic station Emine, and AMSs on 3 October 2025.

	Hourly rain, mm				Three-hourly rain, mm	
	08 UTC	09 UTC	11 UTC	12 UTC	09 UTC	12 UTC
Synop Emine	Not measured		Not measured		34.6	24.0
AMS Nesebar	13.9	14.9	7.2	0.9	29.9	9.2
AMS Beloslav	10.3	12.4	1.1	4.8	30.0	12.0
AMS Sindel	8.4	11.4	1.2	3.9	26.2	10.5

As seen in Figure 9 high density of flashes are detected by MTG LI instrument closely at the location of Cape Emine around 11 UTC. The cloud analyses in Section 3.2 show that this local flash area near Emine is related to a different kind of thunderstorm developed very fast and mostly associated with convective clouds at mid-level, where the thunderstorm process operates mainly. Although only 3-hourly

observations are performed at synoptic station Emine, the data presented in Table 5 can give us information about the significant difference in the precipitation measured in comparison with the other stations, located at some distance.

In the period 09 – 12 UTC, the rain quantity measured at Cape Emine is significantly higher than the other stations considered:

- More than twice at Nesebar (located at a distance of 14 km southwest of the flash area around Emine) as well as at Sindel (located at a distance of 51 km northwest of the area around Emine).
- Twice than at Beloslav (located at a distance of 57 km northwest of the area around Emine).

These heavy precipitations have been accompanied by strong wind gusts of 26 m/s measured at Synoptic station Emine at 1114 UTC close to the time of maximum lightning activity as seen in Figure 9 (c).

These results show that Flash Density parameter in various time intervals provides information to distinguish areas of convection associated with moderate and extreme precipitation as well as wind gusts and thus to anticipate the severity of thunderstorms.

#### **4. CONCLUSIONS**

This study was performed to demonstrate the capabilities of lightning observations as a source of information for monitoring the development of rapidly developing thunderstorms and providing information for the related extreme weather events. Plots of time changes of flash occurrence in time and space are analyzed and their features are related to severe weather reports from ground observations.

Limitations of the method are possible displacements of the weather stations location, at which severe weather events are reported from the storm position in the period of these meteorological observations. The possibility for detailed analyses based on the innovative MTG LI observations is tied by their spatial resolution, which varies within MTG FCI field of view and the sampling distance over central Europe is about 7 km (EUMETSAT, 2025a). Also due to the parallax effect the coordinates of the lightning counts are shifted northeast of area of the real flash area location to a distance of about the cloud top height multiplied by factor of approximately 1.5.

Flash data within various time intervals from 10 to 120 minutes are plotted as single points over satellite imagery. This enables to differentiate older and newer flashes, to observe direction and speed of storm movement, to calculate lightning density in time and space.

In Section 3, examples of monitoring Flash Density and its time changes associated with the development of related thunderstorms are considered. The Flash Density parameter is introduced by the second author of this work taking advantage of Albers equal-area projection used in GEOView software that allows correct calculation of gridded parameters because of the possibility to define "scale factor" of the projection map. This is not applicable for other projection types as Mercator, satellite Geoview or regular latitude/longitude grid, where the map pixel does not have a constant size. The

Flash Density is calculated directly from LFL counts, which are collection of groups (connected LI events on a single acquisition frame) correlated in space. They are averaged on  $2.5 \times 2.5$  km grid of Albers projection for the analyses in Section 3 that is a sub-pixel resolution of MTG LI data, taking into account that sampling distance over Europe of LI instrument is about 7 km (EUMETSAT, 2025 a).

RGB imagery analyses performed in Section 3 shows the position of lightning activity within the convective cloud structure. A case of mid-level thunderstorm clouds with flashes detected by MTG LI instrument near the environment of convective initiation is considered. We hypothesized that this is a case of lower zero-degree isotherm height, so ice particles and graupel drops rapidly formed that is the reason for lightning activity at an early stage of convective development. The results show that Flash Density parameter is sensible to the occurrence of extreme precipitation over the area around the lightning activity. It is shown that flashes occurred especially in convective-cell structures with vertical motions, which enable small ice particles to reach the cloud top as seen in the satellite imagery. Lightning activity may occur just close to the area of convection initiation while flashes are not detected by MTG LI instrument along the downstream development of the storm with mainly large ice crystals seen at the anvil. These results confirm considerations made in EUMETSAT (2025 b).

In Section 2, tracking of thunderstorms is performed with single linear interpolation between start and end positions of the storm. The association of lightning jumps to occurrence of severe weather is still not well confirmed among the community. Considering that identification of lightning jump is a quite difficult task, in Section 2 two different ways of identifying lightning jumps are applied, according to the data from GLD360 measurements:

- Substantial and rapid increase in lightning activity along the track of a thunderstorm cell (Figure 3).
- Significant increasing number of flashes per minute around a specific location averaged from 60 minutes accumulated data, normalized to the number of flashes per minute along a track (Figures 4 and 5).

Further studies are going to be performed applying the methodology presented in Section 2 to explore in more details the association of lightning activity with severe weather in the case considered in Section 3.

The cloud analyses presented in Section 3 demonstrate the capabilities of the GeoView software, developed in Slovak Hydrometeorological Institute (SHMI). This powerful tool, which allows detailed imagery analyses of real-time and archive data has been provided by SHMI and introduced in NIMH for research and operational use.

## **ACKNOWLEDGEMENTS**

This work has been done in international cooperation during the implementation of the Project on Development of the NIMH system for receiving, processing and application of METEOSAT second and third generation data (2022-2025). It is supported by

*Lightning activity seen by GLD360 measurements and MTG satellite observations in relation to occurrence of extreme weather*

EUMETSAT through MTG User Preparation Project and scientific cooperation. The development of GeoView visualization tool with its flexibility, fast application and powerful capabilities to handle high resolution imagery is a merit especially of Mr. Peter Kaňák. Sincere thanks are due to Mr. Peter Kaňák and Mr. Luboslav Okon for their essential support in installation of GEOProc and GeoView software as tools for implementation of the studies, presented in Section 3. The data from the observations of NIMH AWS Nesebar are processed by Mr. Orlin Georgiev for the purposes of the study. Helpful details regarding the observations at synoptic station Emine are given by Ms. Petya Petrova and Ms. Bozhanka Angelova from Meteorological Observatory Burgas. The authors are grateful to the Anonymous Referees for the valuable comments and suggestions that helped significantly refine the manuscript.

## REFERENCES

- DWD (2013) The weather in Germany in June 2013, [https://www.dwd.de/EN/press/press\\_release/EN/2013/20130627\\_DeutschlandwetterimJuni\\_e.pdf?\\_\\_blob=publicationFile&v=5#:~:text=On%2020%20and%2021%20June%2C%20the%20area%20along,just%20over%20the%20long-term%20average%20of%20198%20hours.](https://www.dwd.de/EN/press/press_release/EN/2013/20130627_DeutschlandwetterimJuni_e.pdf?__blob=publicationFile&v=5#:~:text=On%2020%20and%2021%20June%2C%20the%20area%20along,just%20over%20the%20long-term%20average%20of%20198%20hours.)
- EUMETSAT (2025a) MTG LI level 2 data guide, <https://user.eumetsat.int/resources/user-guides/mtg-li-level-2-data-guide>
- EUMETSAT (2025b) Using MTG Lightning Imager (LI) to track convective storms, <https://user.eumetsat.int/resources/user-guides/using-mtg-lightning-imager-li-to-track-convective-storms>
- EUMETSAT CWG (2013) Focus on the most interesting data of the 2.5-minute rapid scan experiments with MSG satellites, <https://cwg.eumetsat.int/2013/10/2-5-minute-rapid-scan-experiments-with-the-msg-satellites>
- Georgiev, C. G., Santurette, P., Maynard, K. (2016). Weather Analysis and Forecasting, 2nd Edition. Applying Satellite Water Vapor Imagery and Potential Vorticity Analysis. ISBN: 978-0-12-800194-3. Academic Press, Elsevier Inc., Amsterdam, Boston, Heidelberg, London, New York, Oxford, Paris, San Diego, San Francisco, Singapore, Sydney, Tokyo. 343pp.
- Georgiev, C, Kanak, J., Holl, G. (2022) Analyses of MTG lightning imager simulated Level 2 data in relation to occurrence of extreme weather events. 2022 EUMETSAT Conference, 19-23 September 2022, Brussels, Belgium. Available online under zip archive named "19-Archimedes" at <https://www.eumetsat.int/media/50259>
- HSAF (2024) Algorithm Theoretical Baseline Document (ATBD) for products P-AC-SEVIRI-PMW (H61B) and P-AC-SEVIRI\_E (H90). Accumulated precipitation at ground by blended MW and IR [https://hsaf.meteoam.it/CaseStudy/GetDocumentUserDocument?fileName=SAF\\_HSAF\\_ATB\\_D-H61-90\\_V2\\_2.pdf&tipo=ATBD](https://hsaf.meteoam.it/CaseStudy/GetDocumentUserDocument?fileName=SAF_HSAF_ATB_D-H61-90_V2_2.pdf&tipo=ATBD)
- Stoyanova, J.S., Georgiev C.G. (2013) SVAT modelling in support to flood risk assessment in Bulgaria. Atmos. Res., 123, pp. 384-399, <http://dx.doi.org/10.1016/j.atmosres.2012.07.002>
- WMO (2025) Recommended WMO standards for RGB composites/recipes from geostationary meteorological imagers. In RGB Experts and Developers Workshop, 1-3 April 2025, Norrköping, Swden, Final Report, FINAL REPORT

Christo Georgiev, Ján Kaňák, Gerrit Holl

<https://wmoomm.sharepoint.com/:b:/s/wmocpdb/EexzMK-JLutNlqR77aiIr8UB2uQvHGE8WfFCq23P03obhQ?e=S9nzet>